

Manuscript Number: MAGMA-D-09-00565

Title: Remarkable crystalline electric field effect and very low-field metamagnetic transition in quasi-two-dimensional antiferromagnet Er<sub>5</sub>Ir<sub>4</sub>Si<sub>10</sub> single crystal without geometrical magnetic frustration

Article Type: Review Article

Keywords: Er<sub>5</sub>Ir<sub>4</sub>Si<sub>10</sub> single crystal, Quasi-two-dimensional antiferromagnet, Low-temperature specific heat under-zero magnetic field, Solid state electro-transport method, Geometrical magnetic frustration, Very low-field metamagnetic transition

Corresponding Author: Dr Kitomi Tsutsumi,

Corresponding Author's Institution:

First Author: Kitomi Tsutsumi

Order of Authors: Kitomi Tsutsumi

Abstract: We have intensively investigated the antiferromagnetic phase transition in the ternary rare-earth metal silicide Er<sub>5</sub>Ir<sub>4</sub>Si<sub>10</sub> single crystal by performing the high-resolution measurement of the low-temperature specific heat under zero-magnetic field and the AC magnetization. In the measurement of important physical quantities associated with the antiferromagnetic phase transition, we have observed anomalies associated with the antiferromagnetic long-range ordering at Neel temperature T<sub>N</sub>. We have confirmed that T<sub>N</sub> is 3.5 K from the high-resolution measurement of the low-temperature specific heat under zero-magnetic field. Furthermore, we have first observed two surprising results. Firstly, a shoulder was observed at about 2K in addition to the sharp peak at T<sub>N</sub>, which is corresponding to the antiferromagnetic transition, in the high-resolution measurement of the low-temperature specific heat. Secondly, the anomaly of the AC magnetization at T<sub>N</sub> depends to the magnetic field direction. We have very clearly observed the

anomaly of the AC magnetization at TN when the AC magnetic field orientation is parallel to the c-axis, whereas we have observed no anomaly of the AC magnetization at TN when the AC magnetic field orientation is perpendicular to the c-axis. These results clarify that our Er<sub>5</sub>Ir<sub>4</sub>Si<sub>10</sub> single crystal is a quasi-two-dimensional antiferromagnet and not a three-dimensional magnetic structure of the Er<sup>3+</sup> local moments. However, we have observed a peak of the AC magnetization around 2K when the AC magnetic field orientation is perpendicular to the c-axis. This temperature corresponds to that at which a shoulder is observed in the measurement of the low-temperature specific heat. Furthermore, we have observed no frequency dependence of the AC magnetization which is ordinarily observed in the spin glass state. This result means that there is no disorder in our Er<sub>5</sub>Ir<sub>4</sub>Si<sub>10</sub> single crystal because the crystal structure of Er<sub>5</sub>Ir<sub>4</sub>Si<sub>10</sub> has the tetragonal crystal structure in which the octagons of the Er<sup>3+</sup> ions are stacked. Both tetragons and octagons of the Er<sup>3+</sup> local moment have no geometrical magnetic frustration. At last we can conclude that both the shoulder of the low-temperature specific heat at about 2K and the peak of the AC magnetization around 2K, which is only observed when the AC magnetic field orientation is perpendicular to the c-axis, correspond to the crystalline electric field effect in the plane which is perpendicular to the c-axis of the tetragonal crystal structure. Furthermore, we report the very low-field metamagnetic transition by applying the DC magnetic field parallel to the c-axis at 2.0 K and the AC magnetic field perpendicular to the c-axis at 1.8 K.

**Dear Editor of JMMM**

**I submit my paper entitled “ Remarkable crystalline electric field effect and very-low field metamagnetic transition in quasi-two-dimensional antiferromagnet  $\text{Er}_5\text{Ir}_4\text{Si}_{10}$  single crystal without geometrical magnetic frustration” to JMMM.**

**With my best regards**

**Dr. Kitomi Tsutsumi  
Department of Physics  
Kanazawa University  
Kanazawa 920-1192  
Japan**

Remarkable crystalline electric field effect and very-low field metamagnetic transition in quasi-two-dimensional antiferromagnet  $\text{Er}_5\text{Ir}_4\text{Si}_{10}$  single crystal without geometrical magnetic frustration

Kitomi Tsutsumi\*

Department of Physics, Kanazawa University, Kanazawa 920-1192, Japan

Abstract

We have intensively investigated the antiferromagnetic phase transition in the ternary rare-earth metal silicide  $\text{Er}_5\text{Ir}_4\text{Si}_{10}$  single crystal by performing the high-resolution measurement of the low-temperature specific heat under zero-magnetic field and the AC magnetization. In the measurement of important physical quantities associated with the antiferromagnetic phase transition, we have observed anomalies associated with the antiferromagnetic long-range ordering at Neel temperature  $T_N$ . We have confirmed that  $T_N$  is 3.5 K from the high-resolution measurement of the low-temperature specific heat under zero-magnetic field. Furthermore, we have first observed two surprising results. Firstly, a shoulder was observed at about 2 K in addition to the sharp peak at  $T_N$ , which is corresponding to the antiferromagnetic phase transition, in the high-resolution measurement of the low-temperature specific heat. Secondly, the anomaly of the AC magnetization at  $T_N$  depends to the magnetic field direction. We have very clearly observed the anomaly of the AC magnetization at  $T_N$  when the AC magnetic field orientation is parallel to the c-axis, whereas we have observed no anomaly of the AC magnetization at  $T_N$  when the AC magnetic field orientation is perpendicular to the c-axis. These results clarify that our  $\text{Er}_5\text{Ir}_4\text{Si}_{10}$  single crystal is a quasi-two-dimensional antiferromagnet and has no three-dimensional magnetic structure of the  $\text{Er}^{3+}$  local moments. However, we have observed a peak of the AC magnetization around 2 K when the AC magnetic field orientation is perpendicular to the c-axis. This temperature corresponds to that at which a shoulder is observed in the measurement of the low-temperature specific heat. Furthermore, we have observed no frequency dependence of the AC magnetization which is ordinarily observed in the spin glass state. This result means that there is no disorder in our  $\text{Er}_5\text{Ir}_4\text{Si}_{10}$  single crystal because the crystal structure of  $\text{Er}_5\text{Ir}_4\text{Si}_{10}$  has the tetragonal crystal structure in which the octagons of the  $\text{Er}^{3+}$  ion are stacked. Both tetragons and octagons of the  $\text{Er}^{3+}$  local moment have no geometrical magnetic frustration. At last we can conclude that both the shoulder of the low-temperature specific heat at about 2 K and the peak of the AC magnetization around 2 K, which is only observed when the AC magnetic field orientation is perpendicular to the c-axis, correspond to the crystalline electric field effect in the plane which is perpendicular to the c-axis of the tetragonal crystal structure. Furthermore, we report the very low-field metamagnetic

transition by applying the DC magnetic field parallel to the c-axis at 2.0 K and the AC magnetic field perpendicular to the c-axis at 1.8 K.

**Keywords:** Er<sub>5</sub>Ir<sub>4</sub>Si<sub>10</sub> single crystal, Quasi-two-dimensional antiferromagnet, Low-temperature specific heat under zero-magnetic field, Solid state electro-transport method, Geometrical magnetic frustration, Crystalline electric field effect, Very low-field metamagnetic transition.

\*Corresponding author. Tel.: +81-76-264-5666; Fax. : +81-76-264-5739

E-mail address: [kitomi@kenroku.kanazawa-u.ac.jp](mailto:kitomi@kenroku.kanazawa-u.ac.jp)

## 1. Introduction

Recently, the ternary rare-earth metal silicide  $R_5Ir_4Si_{10}$  ( $R$  = heavy rare-earth metal, Sc and Lu) have been intensively studied. The attractive phenomena in this ternary compound are antiferromagnetic phase transition [1-8], superconducting phase transition [1, 9-16], charge-density wave phase transition [17-30] and the nuclear magnetism [7]. This compound group crystallizes in the tetragonal  $Sc_5Co_4Si_{10}$ -type crystal structure and the space group is  $P4/mbm$  [1, 7, 16]. The projection of  $Er_5Ir_4Si_{10}$  crystal structure along the  $c$ -axis is shown in Fig. 1. The features of this crystal structure are the absence of the cluster which is composed of the transition metals and the direct bond between the transition metals. These features are in contrast to those of Chevrel phase chalcogenides  $RMo_6S_8$  ( $R$  = rare-earth metal) and rhodium boride compounds  $RRh_4B_4$  ( $R$  = rare-earth metal). In the  $R_5Ir_4Si_{10}$  compound group, the Ir atoms and the Si atoms form planar nets of pentagons and hexagons that are linked in the plain which is perpendicular to the  $c$ -axis and then connected along the  $c$ -axis via Ir-Si-Ir zigzag chains. On the other hand, the rare-earth metal  $R^{3+}$  ions have three sites whose symmetries are different each other. The rare-earth metal  $R^{3+}$  ions at two sites of them make the octagonal layers which are perpendicular to the  $c$ -axis. We must note that the octagonal layer of the rare-earth metal  $R^{3+}$  ions has no magnetic frustration. The rare-earth metal  $R^{3+}$  ions at the third site which are present at the center of the octagons which are composed of Ir atoms and Si atoms also make another layer which is also perpendicular to the  $c$ -axis and a square lattice. We must also note that the square lattice of the  $R^{3+}$  ions has no magnetic frustration. These two layers are perpendicular to the  $c$ -axis, whereas the difference between them is as follows:

The one layer contains only the rare-earth metal  $R^{3+}$  ions and separates the pentagons, hexagon and octagon net works which are composed of Ir atoms and Si atoms. Another layer includes not only the rare-earth metal  $R^{3+}$  ions but also the Ir atoms and Si atoms.

These results mean that there are two kinds of layers which contain the rare-earth metal  $R^{3+}$  ions and perpendicular to the  $c$ -axis. Therefore, we must consider that the character of the  $R_5Ir_4Si_{10}$  compounds is quasi-two-dimensional rather than one-dimensional on the heavy rare-earth metal  $R^{3+}$  ions that correspond to the magnetic properties. Furthermore, all Ir-Si and Si-Si distances are clearly short and indicative of the covalent bonding. In many other ternary rare-earth metal silicides such as  $ThCr_2Si_2$ ,  $CeNiSi_2$  and  $LaRe_2Si_2$ , the net work of the Si atoms and the transition metals exists. In this article, we report and discuss the anomalies in the low-temperature specific heat and the AC magnetization measurements associated with antiferromagnetic long-range ordering in our high-quality  $Er_5Ir_4Si_{10}$  single crystals.

## 2. Experimental

The  $\text{Er}_5\text{Ir}_4\text{Si}_{10}$  single crystals employed in the present study have been grown by Czochoralski pulling method with a tetra-arc furnace in the high purity argon atmosphere whose purity is 6N. The purity of starting materials is as follows. The purity of Si is 6N and that of Ir is 4N. However, the purity of Er is 3N. During the single crystal growth the clear facets have been observed sometimes. We confirmed as-grown crystals to be single crystals by the transmission Laue X-ray photograph method. The single crystals orient along the c-axis. In addition, in order to improve the quality of the as-grown single crystals we used a solid state electro-transport method (SSE). In the SSE process of the as-grown single crystal, we have kept them at 1273 K for a month.

For the measurement of the temperature dependence of the AC magnetization, we have used the commercial Quantum Design SQUID magnetometer (MPMS) from 1.8 to 20 K.

In order to perform the high-resolution measurement of the low-temperature specific heat, a handmade adiabatic method has been employed in the zero-magnetic field because the crystalline electric field effect is an one-ion interaction [31]. This non-commercial apparatus enables us the high-resolution measurement of the low-temperature specific heat down to 0.5 K.

### 3. Results and discussion

In Figs. 2 and 3, we show the temperature dependence of the AC magnetization from 1.8 to 20 K. We show the result in Fig. 2 when the AC magnetic field direction is parallel to the  $c$ -axis and we show the result in Fig. 3 when magnetic field orientation is perpendicular to the  $c$ -axis. When the AC field orientation is parallel to the  $c$ -axis,  $T_N$  is 3.5 K which is precisely consistent with the result of the low-temperature specific heat measurement as is clearly shown in Fig. 4. However, we have no anomaly of the AC magnetization at  $T_N$  when the AC magnetic field direction perpendicular to the  $c$ -axis as is very clearly shown in Fig. 4. When we take the results mentioned just above into consideration, we must conclude that our  $\text{Er}_5\text{Ir}_4\text{Si}_{10}$  single crystals have no three-dimensional magnetic structure of the  $\text{Er}^{3+}$  local moment. This statement is completely different from those which are described in Ref. [18].

In addition, we have observed the peak of the AC magnetization around 2K when the AC magnetic field orientation is perpendicular to the  $c$ -axis. We have already reported that a shoulder is observed in the temperature dependence of the low-temperature specific heat in the vicinity of 2K [7]. A shoulder at about 2K is very precisely consistent with the peak around 2K in the temperature dependence of the AC magnetization when the AC magnetic field orientation is perpendicular to the  $c$ -axis. At last we have completely confirmed that a shoulder corresponds to the magnetic property in the plane which is perpendicular to the  $c$ -axis of  $\text{Er}_5\text{Ir}_4\text{Si}_{10}$  single crystal. This result reveals that  $\text{Er}_5\text{Ir}_4\text{Si}_{10}$  single crystal is a quasi-two-dimensional material and a quasi-two-dimensional antiferromagnet.

Next, we must discuss on the relation between a shoulder in the temperature dependence of the low-temperature specific heat at about 2 K and the peak of the AC magnetization around 2 K when the AC magnetic field orientation is perpendicular to the  $c$ -axis. A shoulder suggests that the magnetic spatial ordering is a short-range one. The representative magnetic short-range ordering is the spin glass state. The AC magnetization measurement is very powerful for the investigation of the spin glass behavior. We have performed the frequency dependence measurement of the AC magnetization by using the AC magnetic field whose orientation is perpendicular to the  $c$ -axis. The results are shown in Fig. 5. We have observed no spin glass like behavior. Namely, the peak of the AC magnetization does not shift to higher temperature and the AC magnetization rapidly decreases with increasing the frequency of the AC magnetic field. These results means that there is no spin glass state in our  $\text{Er}_5\text{Ir}_4\text{Si}_{10}$  single crystal. Non-existence of the spin glass state verifies that there is no disorder in our SSE processed  $\text{Er}_5\text{Ir}_4\text{Si}_{10}$  single crystal because the crystal structure of  $\text{R}_5\text{Ir}_4\text{Si}_{10}$  ( $\text{R} = \text{Tb}, \text{Dy}, \text{Ho}, \text{Er}$ ) has no geometrical magnetic frustration. Therefore, we can conclude that a shoulder at about 2 K in the temperature dependence of the low-temperature specific heat and the peak of the AC magnetization when the AC magnetic field orientation is perpendicular to the  $c$ -axis originate from the crystalline electric field effect in the plane of  $\text{Er}_5\text{Ir}_4\text{Si}_{10}$  single crystal which is



perpendicular to the c-axis.

Galli et al. [16-18] had reported that the high-quality single crystal of  $\text{Er}_5\text{Ir}_4\text{Si}_{10}$  single crystal undergoes the long-range antiferromagnetic transition at 2.8 K from the DC magnetization measurement by using Quantum Design MPMS, the measurements of the resistivity and the specific heat by Quantum Design PPMS and the neutron diffraction study. These measurements by using Quantum Design MPMS and PPMS only down to 1.8 K cannot clearly detect a *shoulder* in the low-temperature specific heat [7] and the AC magnetization peak around 2 K which we have first observed and reported in this article. We strongly insist that the original finding mentioned just above originates from the high quality of our SSE processed single crystals. In fact,  $T_N$  is 3.5 K of our samples, whereas  $T_N$  of the high-quality single crystal prepared by Galli et al. is 2.8 K which is lower than our  $T_N$ . Furthermore, we show the temperature dependence of the low-temperature specific heat of our as-grown single crystal in Fig. 6. We have clearly observed two successive peaks. This observation in the temperature dependence of the low-temperature specific heat is very comparable with that of  $\text{Yb}_5\text{Ir}_4\text{Si}_{10}$  polycrystalline sample which is reported in Ref. [28]. But we have clearly observed a shoulder around 2 K together with the sharp peak at  $T_N = 3.5$  K in our SSE processed  $\text{Er}_5\text{Ir}_4\text{Si}_{10}$  single crystal.

On the other hand, G. J. Li et al. have reported on the superconductivity of  $\text{Sc}_5\text{Ir}_4\text{Si}_{10}$  single crystal grown by the floating zone method [14]. Those single crystals have clearly showed anisotropic superconducting properties which are very well explained in the standard BCS model. Furthermore, we must note that the observation of the peak effect in the superconducting state is the direct evidence of the quasi-two-dimensional character of the crystal structure [33]. The observation of the peak effect in  $\text{Sc}_5\text{Ir}_4\text{Si}_{10}$  single crystal grown by the floating method is very consistent with our study of the antiferromagnetic properties of our SSE processed  $\text{Er}_5\text{Ir}_4\text{Si}_{10}$  single crystal grown by Czochoralski pulling method by using a tetra-arc furnace under high purity argon atmosphere. Furthermore, we have precisely measured the metamagnetic transition when the DC magnetic field orientation is parallel to the c-axis. As is very clearly shown in Fig. 7, we have observed the metamagnetic transition in the magnetic field above 1000 Oe at 2.0 K. When the AC magnetic field orientation is perpendicular to the c-axis, we have very clearly observed the hysteresis loop of the AC magnetization around 1350 Oe at 1.8 K as is shown in Fig. 8.

#### 4. Conclusion

The experimental results of the low-temperature specific heat down to 0.5 K under zero-magnetic field combined with the AC magnetization measurement down to 1.8 K in the SSE processed  $\text{Er}_5\text{Ir}_4\text{Si}_{10}$  single crystals have revealed the experimental evidences for the following conclusions.

- (1)  $\text{Er}_5\text{Ir}_4\text{Si}_{10}$  single crystal is a quasi-two-dimensional material.
- (2)  $\text{Er}_5\text{Ir}_4\text{Si}_{10}$  single crystal is a quasi-two-dimensional antiferromagnet.
- (3)  $\text{Er}_5\text{Ir}_4\text{Si}_{10}$  single crystal exhibits an antiferromagnetic long-range ordering in the plane perpendicular to the c-axis of the tetragonal crystal structure, whereas there is no three-dimensional magnetic structure of the  $\text{Er}^{3+}$  local moments.
- (4) The remarkable crystalline electric field effect is only observed in the plane which is perpendicular to the c-axis of the tetragonal crystal structure.
- (5) In order to clarify the intrinsic magnetic properties, we need the high-resolution measurement of the low-temperature specific heat under zero-magnetic field together with the high-resolution measurement of the magnetization.
- (6) In the SSE processed quasi-two-dimensional antiferromagnet  $\text{Er}_5\text{Ir}_4\text{Si}_{10}$  single crystal without geometrical magnetic frustration, we have very clearly observed the very low-field metamagnetic transition.
- (7) The SSE process is indispensable in order to clarify the intrinsic magnetic properties of the single crystals grown by Czochralski pulling method because the SSE process improves the quality of the as-grown single crystals.
- (8) Finally, we strongly insist that the structural phase transition of  $\text{Lu}_5\text{Ir}_4\text{Si}_{10}$  single crystal is much the same as the cubic-tetragonal phase transition in A15 compounds because the nature of the phase transition in both compounds is the first-order one [10,24,33].

## References

- [1] Ternary Superconductors, edited by G. K. Shenoy, B. D. Dunlap, F. Y. Fradin, Elsevier North Horland, Amsterdam, The Netherland, 1981.
- [2] S. Ramakrishnan, K. Gosh, Girish Chandra, *Phys. Rev. B* 45 (1992) 10769.
- [3] S. Ramakrishnan, K. Gosh, Girish Chandra, *Phys. Rev. B* 46 (1992) 2958.
- [4] K. Gosh, S. Ramakrishnan, Girish Chandra, *Phys. Rev. B* 48 (1993) 4152.
- [5] S. Ramakrishnan, K. Gosh, Aravind D. Chnchure, Kristian Jonason, V. R. Marathe, Girish Chandra, *Phys. Rev. B* 51 (1995) 8398.
- [6] K. Katoh, T. Tsutsumi, K. Yamada, G. Terui, Y. Niide, A. Ochiai, *Physica B* 373 (2006) 111.
- [7] K. Tsutsumi, S. Takayanagi, K. Maezawa, H. Kitazawa, *J. Alloys Comp.* 453 (2008) 55.
- [8] K. Tsutsumi, S. Nimori, G. Kido, *J. Alloys Comp.* 470 (2009) 1.
- [9] L. S. Hausermann-Berg, R. N. Shelton, *Phys. Rev. B* 35 (1987) 4673.
- [10] L. S. Hausermann-Berg, R. N. Shelton, *Phys. Rev. B* 35 (1987) 6659
- [11] H. D. Yang, R. N. Shelton, H. F. Braun, *Phys. Rev. B* 33 (1986) 5062.
- [12] R. N. Shelton, L. S. Hausermann-Berg, P. Klavins, H. D. Yang, M. S. Anderson, C. A. Swenson, *Phys. Rev. B* 34 (1986) 4590.
- [13] T. Koyama, H. Sugita, S. Wada, K. Tsutsumi, *J. Phys. Soc. Jpn.* 68 (1999) 2326.
- [14] G. J. Li, M. Miura, Z. X. Shi, T. Tamegai, *Physica C* 463-465 (2007) 76.
- [15] H. F. Braun, C. U. Segre, *Solid State Commun.* 35 (1980) 735.
- [16] H. F. BRAUN, K. YVON, R. M. BRAUN, *Acta Crystallogr. B* 36 (1980) 2397.
- [17] F. Galli, T. Taniguchi, A. A. Menovsky, G. J. Nieuwenhuys, J. A. Mydosh, S. Ramakrishnan, *Physica B* 281&282 (2000)171.
- [18] F. Galli, S. Ramakrishnan, T. Taniguchi, G. J. Nieuwenhuys, J. A. Mydosh, S. Geupel, J. Ludecke, S. van Smaalen, *Phys. Rev. Lett.* 85 (2000) 158.
- [19] F. Galli, R. Feyerherm, R. W. A. Hendrix, S. Ramakrishnan, G. J. Nieuwenhuys, J. A. Mydosh, *Phys. Rev. B* 62 (2000) 13840.
- [20] Yogesh Singh, S. Ramakrishnan, *Physica B* 359-361 (2005) 494.
- [21] M. H. Jung, H. C. Kim, A. Migliori, F. Galli, J. A. Mydosh, *Phys. Rev. B* 68 (2003) 132102.
- [22] H. D. Yang, P. Klavins, R. N. Shelton, *Phys. Rev. B* 43 (1991) 7688.
- [23] Sander van Smaalen, Mohammad Shaz, Lukas Palatinus, Peter Daniels, Federica Galli, Gerard J. Nieuwenhuys, J. A. Mydosh, *Phys. Rev. B* 69 (2004) 014103.
- [24] B. Becker, N. G. Patil, S. Ramakrishnan, A. A. Menovsky, G. J. Nieuwenhuys, J. A. Mydosh, M. Kohgi, K. Iwasa, *Phys. Rev. B* 59 (1999) 7266.
- [25] J. B. Betts, A. Migliori, G. S. Boebinger, H. Ledbetter, F. Galli, J. A. Mydosh, *Phys. Rev. B* 66 (2002) 060106.
- [26] Y. K. Kuo, Y. Y. Chen, L. M. Wang, H. D. Yang, *Phys. Rev. B* 69 (2004) 235114.

- [27] Y. K. Kuo, F. H. Hsu, H. H. Li, H. I. Haung, C. W. Haung, C. S. Lue, H. D. Yang, *Phys. Rev. B* **67** (2003) 195101.
- [28] Z. Hossain, M. Schmidt, W. Schnelle, H. S. Jeevan, C. Geibel, S. Ramakrishnan, J. A. Mydosh, Y. Grin, *Phys. Rev. B* **71** (2005) 060406.
- [29] S. Ramakrishnan, J. A. Mydosh, *J. Magn. Magn. Mater.* **310** (2007) 207.
- [30] F. Galli, G. J. Nieuwenhuys, D. E. MacLaughlin, R. H. Heffner, A. Amato, O. O. Bernal, J. A. Mydosh, *Physica B* **319** (2002) 282.
- [31] D. Gignoux, D. Schmitt, *J. Alloys Comp.* **326** (2001) 143.
- [32] H. A. Radovan, N. A. Fortune, T. P. Murphy, S. T. Hannahs, E. C. Palm, S. W. Tozer, D. Hall, *Nature* **425** (2003) 51.
- [33] B. T. Matthias, T. H. Geballe, V. B. Compton, *Rev. Mod. Phys.* **35** (1963) 1.

### Figure captions

**Fig. 1.** Projection of  $\text{Er}_5\text{Ir}_4\text{Si}_{10}$  crystal structure along the c-axis which is  $\text{Sc}_5\text{Co}_4\text{Si}_{10}$ -type tetragonal one. Filled circles correspond to  $z = 0, 1$  and open circles to  $z = 1/2$  where  $z$  is the fractional coordinate along the c-axis of the tetragonal crystal structure.

**Fig. 2.** Temperature dependence of the AC magnetization in  $\text{Er}_5\text{Ir}_4\text{Si}_{10}$  single crystal when the AC magnetic field orientation is parallel to the c-axis. We must note that there is no anomaly of the AC magnetization around 2K.

**Fig. 3.** Temperature dependence of the AC magnetization in  $\text{Er}_5\text{Ir}_4\text{Si}_{10}$  single crystal when the AC magnetic field orientation is perpendicular to the c-axis. We must note that there is no anomaly of the AC magnetization at  $T_N = 3.5$  K.

**Fig. 4.** Temperature dependence of the low-temperature specific heat under zero-magnetic field in our SSE processed  $\text{Er}_5\text{Ir}_4\text{Si}_{10}$  single crystal.

**Fig. 5.** Frequency dependency of the AC magnetization when the magnetic field orientation is perpendicular to the c-axis. The measurements have been performed at 1.0, 10, 100 and 1000 Hz, respectively. No spin glass behavior has observed. We must note that no spin glass behavior clarifies that there is no disorder in our SSE processed  $\text{Er}_5\text{Ir}_4\text{Si}_{10}$  single crystal.

**Fig. 6.** Temperature dependence of the low-temperature specific heat in the as-grown  $\text{Er}_5\text{Ir}_4\text{Si}_{10}$  single crystal grown by Czochoralski pulling method. We must note that two successive peaks are clearly observed.

**Fig. 7.** The metamagnetic transition of the quasi-two-dimensional antiferromagnet  $\text{Er}_5\text{Ir}_4\text{Si}_{10}$  single crystal by applying the DC magnetic field parallel to the c-axis at 2.0 K. We must note that the metamagnetic transition occurs in the very low-field, namely, about 1000 Oe.

**Fig. 8.** The metamagnetic transition of the quasi-two-dimensional antiferromagnet  $\text{Er}_5\text{Ir}_4\text{Si}_{10}$  single crystal by applying the AC magnetic field perpendicular to the c-axis at 1.8 K. We must note that the hysteresis loop of the AC magnetization around 1350 Oe has been very clearly observed.

Figure 1

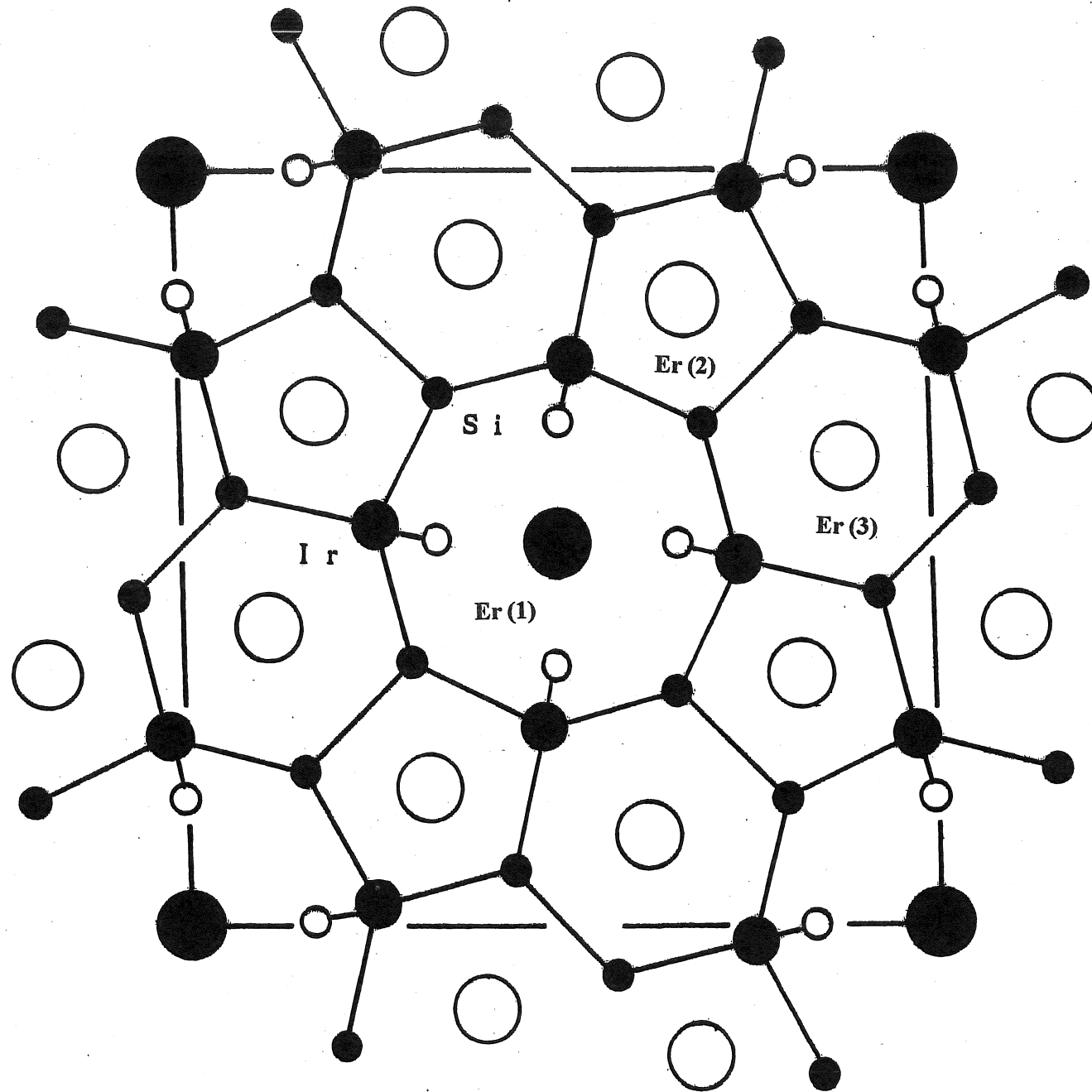


Figure 2

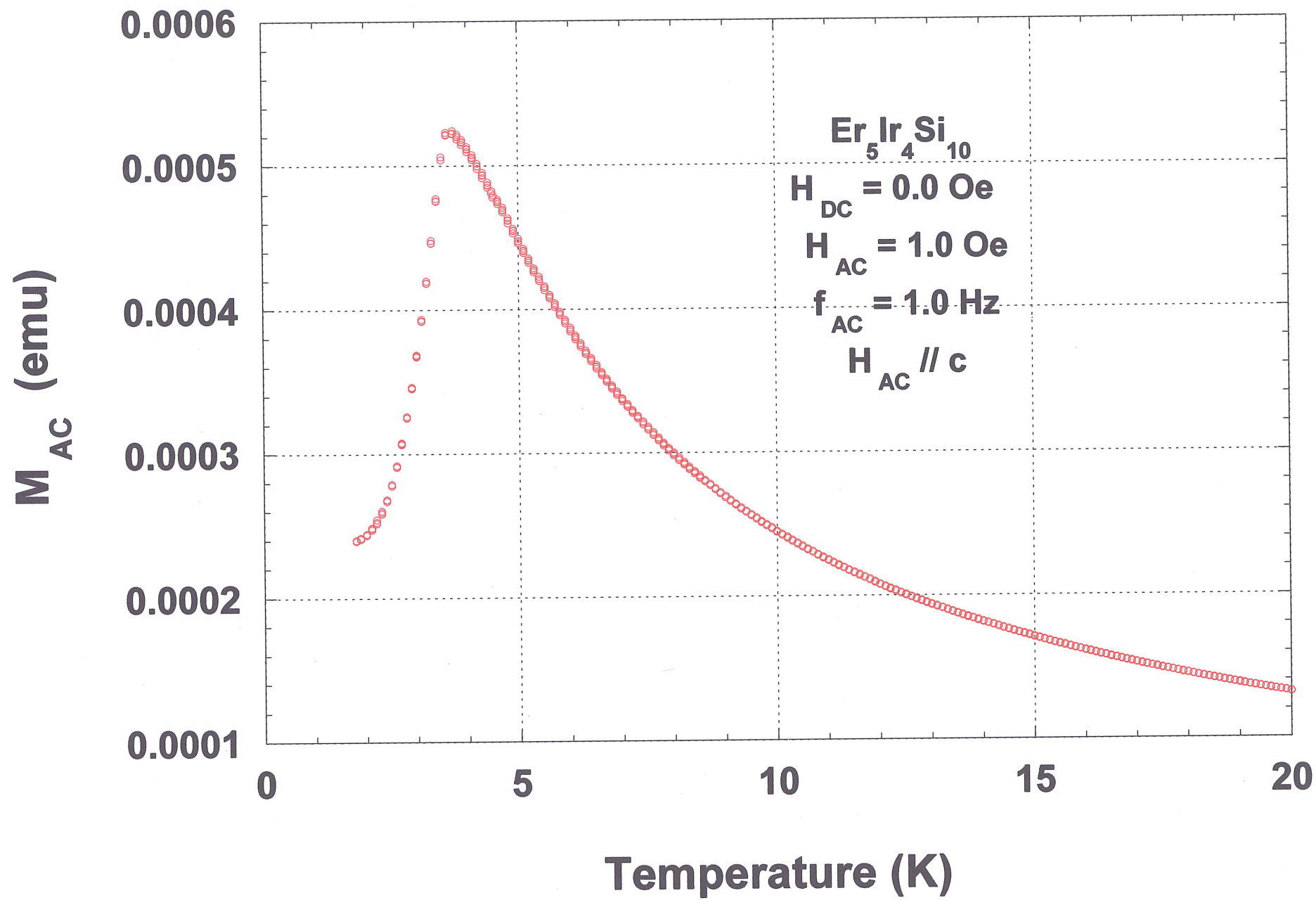


Figure 3

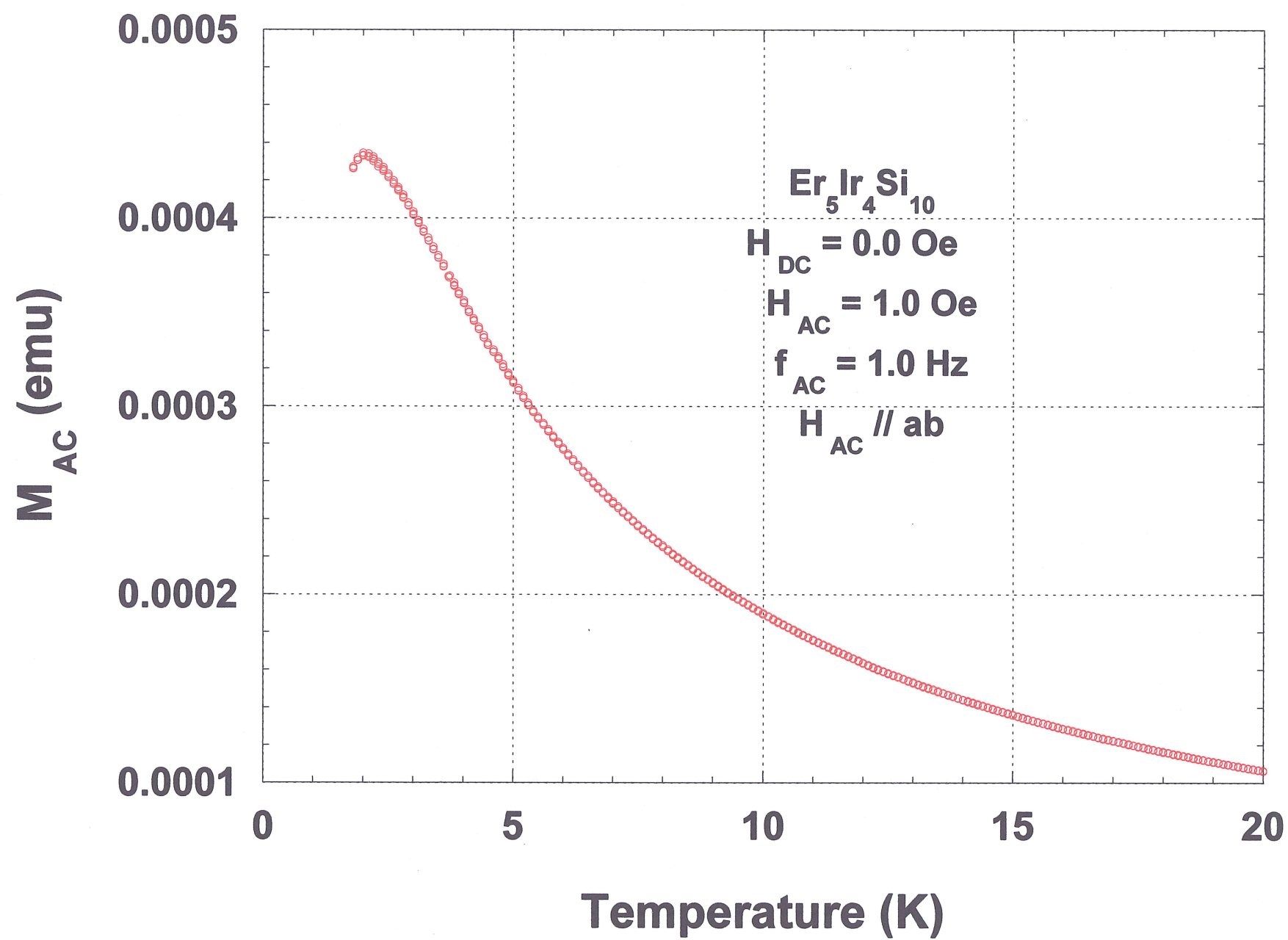




Figure 4

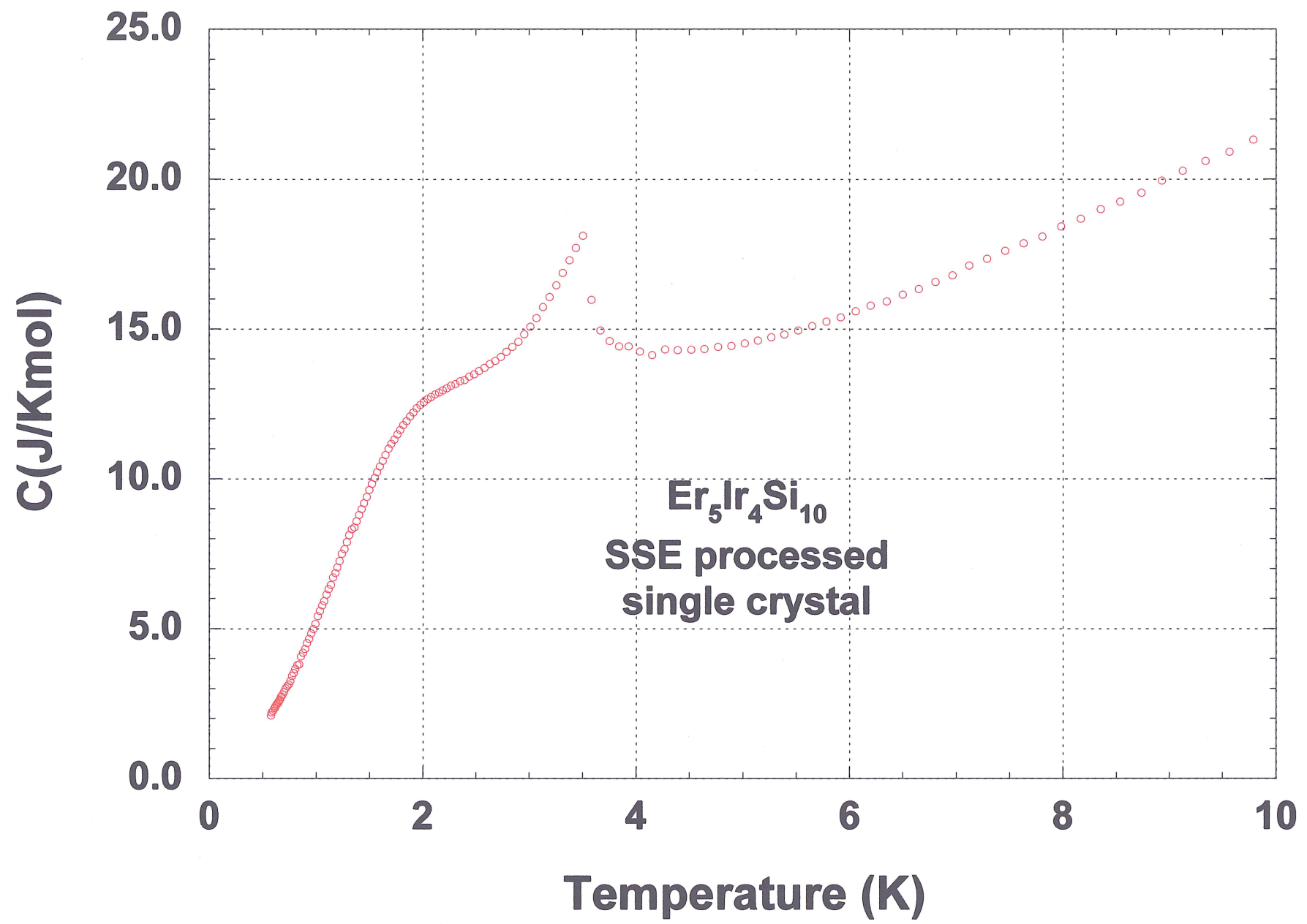


Figure 5

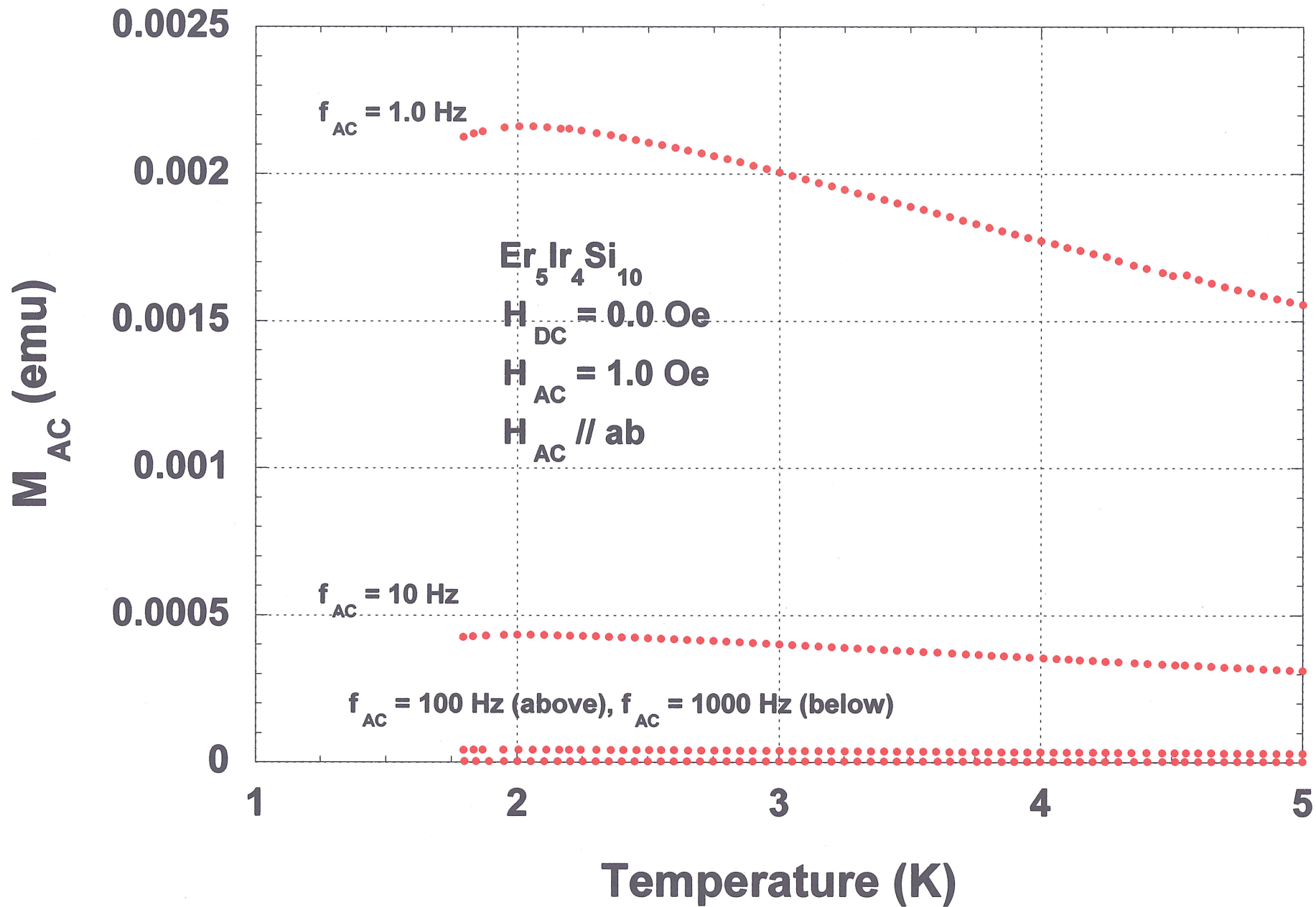


Figure 6

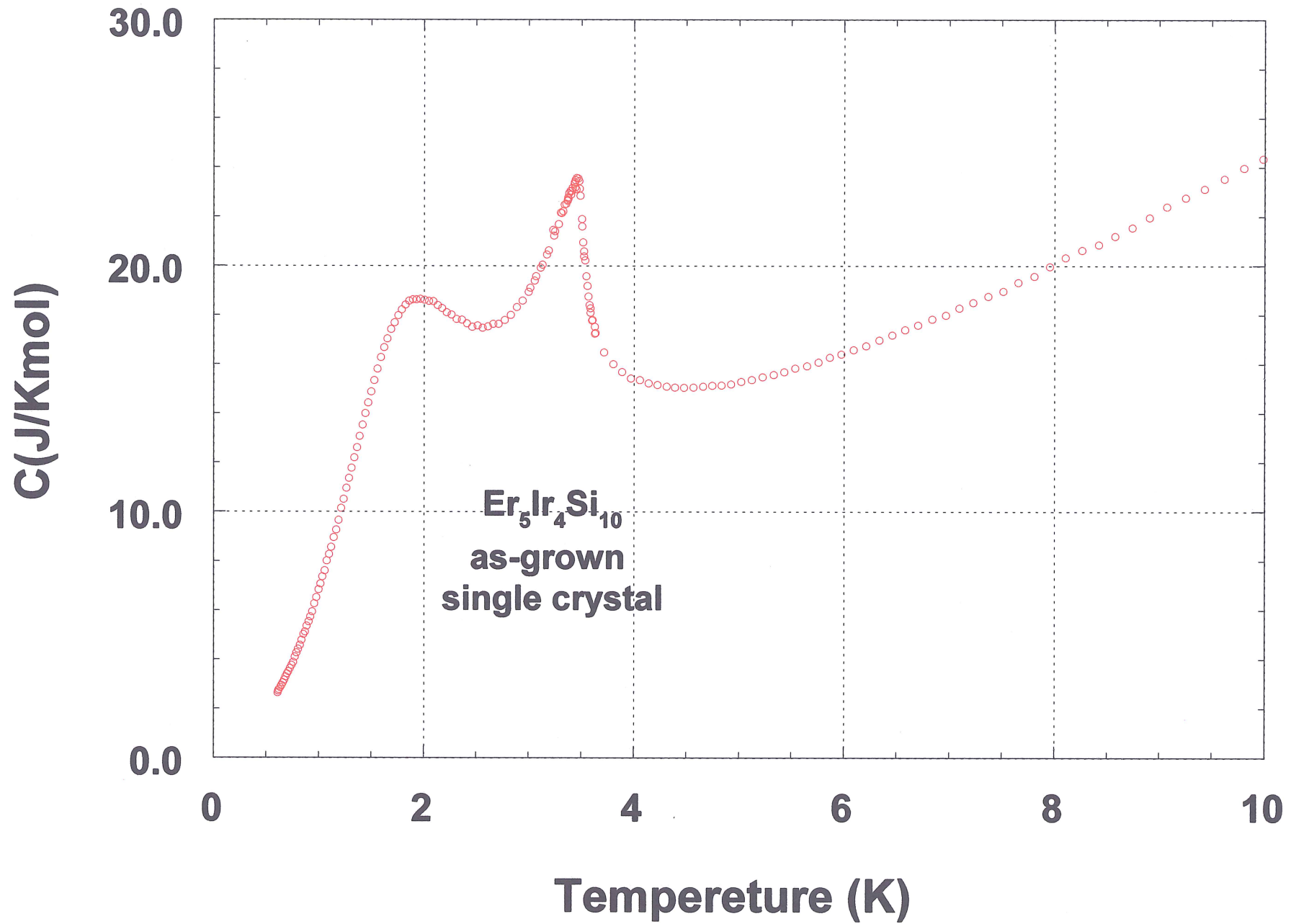


Figure 7

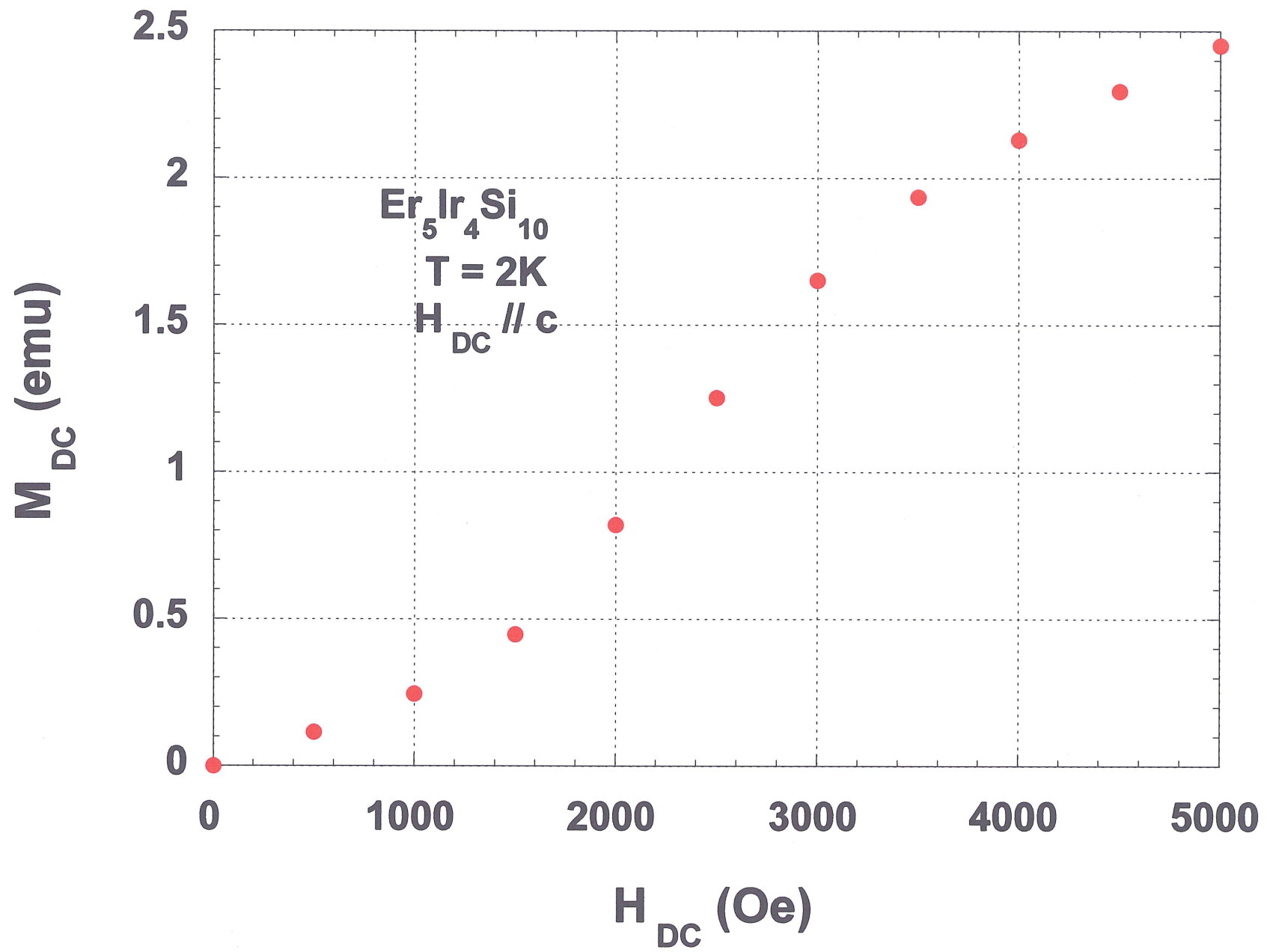


Figure 8

